

Supporting Energy harvesting efficiency in GaN nanowires based nanogenerators: the critical influence of the Schottky nanocontact

Nicolas Jamond, et al.

Supporting S1: AFM-Resiscope - Configurations for electrical measurements

One of the most common methods to measure the piezoelectric effect in NWs consists in involving lateral bending or vertical compression of the nanostructure with simultaneous measurement of generated electric potential. This method requires a very sensitive measurement system, since the generated voltages and currents tend to be small when a single NW is tested. In this work, the electrical measurements were performed by an AFM equipped with a modified Resiscope module [s1,s2]. The AFM technique brings the advantage of the scanning and deflection measurements capabilities with a nanometer scale resolution. The Resiscope, which in its standard form allows dynamic resistance measurements over a very wide range (10^2 – 10^{12} Ω) in usual AFM scanning conditions, has been adapted in order to allow investigations on piezoelectric properties of NW [s1,s3].

The electrical module is connected to the substrate and to the conductive AFM tip. At the substrate/nanostructure interface, an Ohmic contact is formed [s4], while the GaN NW top/AFM tip contact forms a Schottky diode, a prerequisite to harvest the piezoelectric energy.

Piezoelectric conversion measurements: In this specific instrumental configuration (Fig. S1), the AFM is used in scanning configuration. During scanning over the array of vertical NWs, the conductive AFM tip is brought into contact with the surface under a controlled and constant normal force. This normal force combined with the lateral one resulting from the scanning movement of the tip, induces a local bending of the nanostructures. In response to this deflection and due to the piezoelectric properties of wurtzite GaN materials, the NWs generate a voltage which is detected through the conductive AFM tip. Throughout the measurements, both the topographic and the electrical signals are recorded continuously and simultaneously, no external voltage being applied during the measurement. The voltage waveform generated by the NW is observed across a load resistance R_L of 1 G Ω .

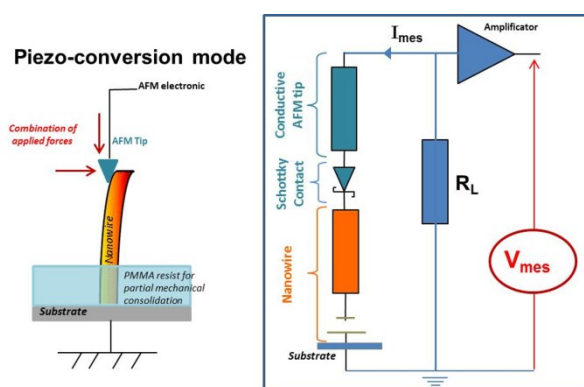


Fig. S1: Schematic representation of the AFM system equipped with a modified-Resiscope module in piezo-conversion configuration.

Current-voltage measurements: In this instrumental configuration (Fig. S2), the AFM is used in vertical mode. The AFM tip is brought into contact with the NW top and induces a vertical compression of the nanostructures under a controlled and constant normal force. The voltage is applied via the substrate and the current is collected through the conductive AFM tip. We have thus a negative representation of the diode characteristic. When the contact is negatively polarized ($V_{\text{Bias}} = V_{\text{GaN NWs}} - V_{\text{Tip}} < 0$), the forward current is able to cross the interface. By contrast, when the AFM tip - GaN NW contact is submitted to positive polarization ($V_{\text{Bias}} = V_{\text{GaN NWs}} - V_{\text{Tip}} > 0$), the reverse current is blocked by the diode, leading to a weak current.

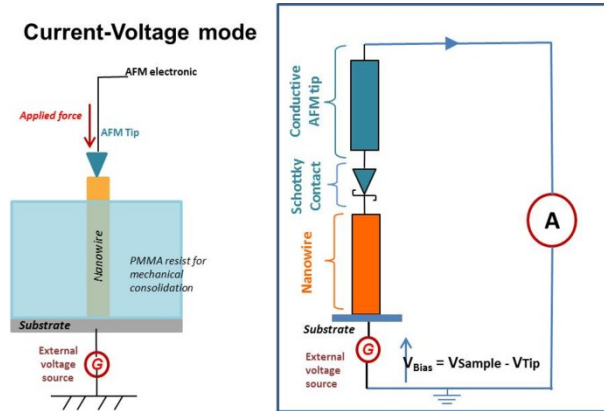


Fig. S2: Schematic representation of the AFM system equipped with a modified-Resiscope module in current-voltage configuration.

- [s1] N. Gogneau, P. Chretien, E. Galopin, S. Guilet, L. Travers, J.-C. Harmand, F. Houz , *Phys. Status Solidi RRL* 2014, **8**, 414.
- [s2] O. Schneegans, P. Chretien, F. Houze, French patent FR 10 01940, (5 May 2010), international PCT WO 2011/138738, (10 November 2011).
- [s3] N. Gogneau, P. Chretien, E. Galopin, S. Guilet, L. Travers, J.-C. Harmand, F. Houz , *Appl. Phys. Lett.* 2014, **104**, 213105.
- [s4] G. Jacopin, A. De Luna Bugallo, L. Rigutti, P. Lavenus, F. H. Julien, Y. T. Lin, L. W. Tu, M. Tchernycheva, *Appl. Phys. Lett.* 2014, **104**, 023116.

Supporting S2: Characteristics of the AFM tips

The table S2 presents the characteristics of the three conductive AFM tips used to investigate the piezoelectric properties of the GaN NWs. Because the work function of each tested conductive AFM tip ($W_{\text{p-type doped diamond}} \sim 5.21$ eV, $W_{\text{SiPt}} \sim 5.03$ eV and $W_{\text{Pt/Ir}} \sim 5.13$ eV) are superior to the electron affinity of the GaN (4.1 eV [s5]), the metal–GaN contact forms a Schottky barrier that ensures the charge recuperation for piezo-generation [s6].

	p-type doped diamond	PtSi	Pt/Ir
Work function [eV]	5.21	5.03	5.13
Tip radius [nm]	144 ± 2	25 ± 2	21 ± 2
Nominal spring constant [N/m] for conversion measurements	0.3	2	2
Nominal spring constant [N/m] for I-V measurements	0.2	0.2	0.2

Table S1: Characteristics of the conductive AFM tips

Determinations of an AFM tip work function:

The work function of a conductive AFM tip is not a characteristic commonly found in the literature. For each AFM tip, the wide value dispersion reported for its coating material makes difficult the choice of relevant values to use in our discussion. In order to avoid to choose randomly these values, we have measured the work function of each conductive AFM tip used in this work.

The work function of a conductive AFM tip can be determined by imaging the surface potential (SP) of a sample with a known work function. The SP mode, also named Kelvin mode, is an AFM experimental technique, which has been demonstrated as a powerful tool for measuring electric potential distribution with nanometer resolution [s7]. This technique detects the interactions between the conductive tip and the sample through long-range Coulomb forces to create the SP image. SP mapping of the surface was achieved in lift mode with a lift scan height of 15 nm.

The surface potential is related to the work function required to move an electron from the material to the vacuum. It is significant for each material and can be defined as:

$$q \cdot SP^{measured} = W_{tip} - W_{sample} \quad (1)$$

where W_{tip} and W_{sample} are respectively the work functions of the tip and the sample, and q is the elementary charge [s8, s9].

We have imaged the surface potential of a 250 nm-thick Gold layer deposited on a carrier substrate. The figure S3a presents the SP images performed in the same conditions of the gold surface with the three conductive AFM tips. The corresponding surface potential profiles through the x-axis are shown on Fig. 3b. According to the eq. 1 and knowing that the work function of a thin gold layer deposited on host substrate is equal to 5.3 eV according to reference [s10], we found the following work functions:

$$\begin{aligned} W_{\text{p-type doped diamond}} &\sim 5.21 \text{ eV,} \\ W_{\text{SiPt}} &\sim 5.03 \text{ eV} \\ W_{\text{Pt/Ir}} &\sim 5.13 \text{ eV} \end{aligned}$$

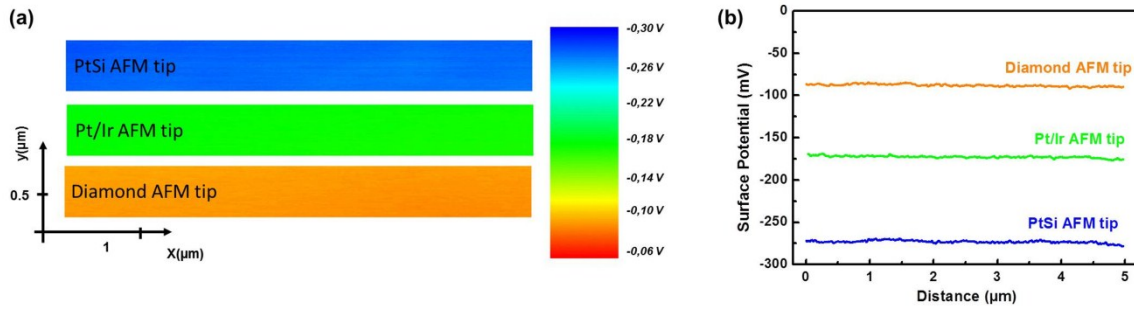


Fig. S3: (a) Surface Potential mapping of our reference gold surface for the p-type doped diamond, PtSi and Pt/Ir AFM tips and (b) the corresponding surface potential profiles through the x-axis.

AFM tip radius:

In order to know the tip radius of each conductive AFM tip used in our experiments, we have imaged them by scanning electron microscope in lateral view. The figure S4 presents the SEM and coloured images of the diamond (Fig. S4a-b), PtSi (Fig. S4c-d) and Pt/Ir (Fig. S4e-f) AFM tips.

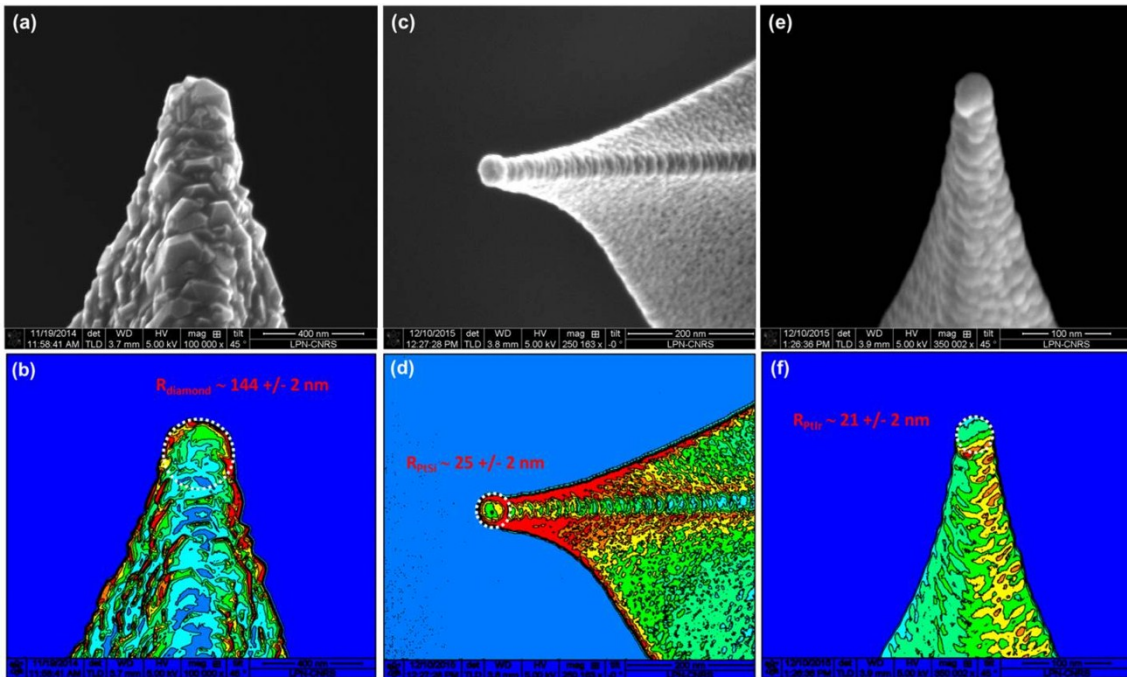


Fig. S4: SEM and coloured images of Diamond (a-b), PtSi (c-d) and PtIr (e-f) conductive AFM tips. The white dashed circle is a eyes guide.

[s5] V. Bougrov, M.E. Levinshtein, S. L. Rumyantsev, A. Zubrilov, Properties of Advanced Semiconductor Materials: GaN, AlN, InN, BN, SiC, SiGe, Wiley: New York **2001**, 1
[s6] J. Liu, P. Fei, J. Song, X. Wang, C. Lao, R. Tummala, Z. L. Wang, *Nano Lett.* 2008, **8**, 328.
[S7] N. Gogneau, A. Balan, M. Ridene, A. Shukla, A. Ouerghi, *Surf. Sci.* 2012, **606**, 217.
[S8] Y-J. Yu, Y. Zhao, S. Ryu, L. E. Brus, K. S. Kim, P. Kim, *Nano Lett.* 2009, **9**, 3430.
[S9] Y. Rosenwaks, R. Shikler, Th. Glatzel, S. Sadewasser, *Phys. Rev. B* 2004, **70**, 085320.
[S10] W. M. H. Sachtler, G. J. H. Dorgelo, A. A. Holscher, *Suf. Sci.* 1966, **5**, 221.

Supporting S3: Piezoelectric energy nanogeneration

The table S3 summarizes the average output voltages and power densities generated by GaN NWs for a constant normal tip force of 20 ± 5 nN, 50 ± 5 nN and 90 ± 8 nN, and for the three tested conductive AFM tip/GaN NWs Schottky contacts. The average output voltages have been measured from the statistical analysis of the 3D electrical mappings, and the average power densities have been calculated by using the following equation: $P = \frac{\overline{V_i^2}}{R_L} \cdot \rho$, where V_i is the output voltage generated by the i -th NW, R_L is the resistance across which the measurement is performed ($1G\Omega$) and ρ is the surface density of NWs.

Conductive AFM tip Constant normal force (nN)	p-type doped diamond		PtSi		Pt/Ir	
	Average output voltage (mV)	Average power density (mW/cm ²)	Average output voltage (mV)	Average power density (mW/cm ²)	Average output voltage (mV)	Average power density (mW/cm ²)
20 ± 5	-98 ± 100	9.2 ± 2.8	-222 ± 21	29.6 ± 5.7	-231 ± 16	41.7 ± 4.9
50 ± 5	-152 ± 71	19.1 ± 17	-219 ± 28	38.6 ± 8.2	-236 ± 10	49.0 ± 10.2
90 ± 8	-196 ± 37	29.7 ± 10.4	-226 ± 20	40.3 ± 3.0	-234 ± 6	47.1 ± 3.0

Table S2: Average values and standard deviations (with a measurement precision of 2%) of the output voltages and average power density generated by GaN NWs for a constant normal tip force of 20 ± 5 nN, 50 ± 5 nN and 90 ± 8 nN, and for the three tested conductive AFM tip/GaN NWs Schottky contacts.

Supporting S4: Calculation of the contact surface between the GaN NW and the conductive AFM tip.

In order to estimate the size of the contact between the AFM tip (the end of the tip is assumed to be equivalent to a half-sphere) and the surface of the GaN nanowire, we are using the Hertz's theory [s11]. This theory describes a regime of purely elastic deformation between two perfectly smooth solids, in the absence of adhesion and friction. In these conditions, the mechanical contact between a sphere of radius R (here the AFM tip radius) and a plane (here the GaN top NW) is expressed as a disk of radius a by the following eq.:

$$a = \left(\frac{3}{4} \frac{F R}{E^*} \right)^{1/3} \quad (2)$$

where F is the applied force, R is the AFM tip radius measured by scanning electronic microscope (supporting S2) and E^* is the reduced Young's modulus of the two materials (the conductive AFM tip and the GaN NWs) and given by:

$$\frac{1}{E^*} = \left(\frac{1-\nu_1^2}{E_1} \right) + \left(\frac{1-\nu_2^2}{E_2} \right) \quad (3)$$

E_1 , E_2 and ν_1 , ν_2 are respectively the Young's modulus and Poisson's ratios of the two materials.

The materials settings considered for the calculations are presented into the table S3

	GaN	Diamond	PtSi	PtIr
Young's modulus E (GPa)	300* [s12]	1063 [s13]	238 [s14]	233 [s15]
Poisson coefficient ν	0.25 / 0.4 [s16]	0.1 [s13]	0.32 [s14]	0.37 [s15]
Tip radius R (nm)		144	25	21

Table S3: Materials settings used for the calculations
(*GaN bulk value)

The figure S5 presents the evolution of the calculated radius a of the contact surface as a function of the applied force (evolving between 1 and 100 nN) for the three AFM tips.

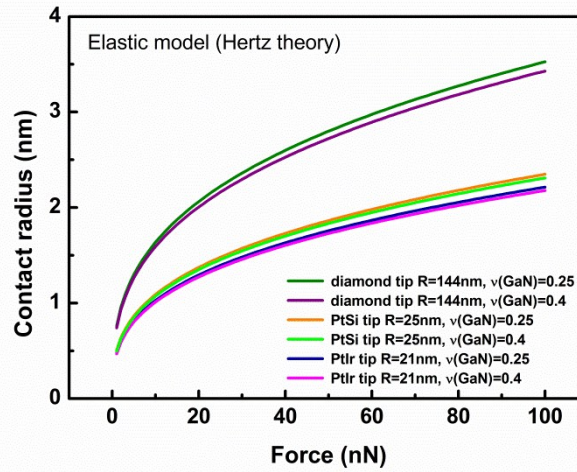


Fig. S5: Evolution of the contact radius of the Schottky diode for each conductive AFM tip as a function of the applied force

[s11] K.L. Johnson, *Contact Mechanics*, Cambridge University Press, Cambridge, **1989**.

[s12] R.A. Bernal, R. Agrawal, B. Peng, K.A. Bertness, N.A. Sanford, A.V. Davydov, H. D. Espinosa, *Nano Lett.* 2011, **11**, 548.

[s13] A.V. Eletskii, *Physics – Uspekhi* 2007, **50**, 225.

[s14] H. Koca, E. Deligözb, A.M. Mamedovc, *Phil. Mag. A* 2011, **91**, 3093.

[s15] J. Merker, D. Lupton, M. Töpfer, H. Knake, *Platinum Metal Rev.* 2001, **45**, 74.

[s16] F. Glas, B. Daudin, *Phys. Rev. B* 2012, **86**, 174112.

Supporting S5: Relation between the Schottky nanocontact and the energy harvesting efficiency.

The quantification of the ideality factor (n), the series resistance (R_S) and the effective Schottky barrier height (SBH) allows us to discuss the influence of the AFM tip-GaN NW Schottky nanocontact on the energy harvesting efficiency.

The thermionic emission theory [s17]:

In this approach, an ideal Schottky diode is assumed and thus the series resistance is neglected. The current-voltage relationship, for $V \gg k_B T/q$, is given by the eq.:

$$I = I_S \exp\left(\frac{qV}{nk_B T}\right) \quad (4)$$

where, in our case, V is $-V_{Bias}$ and I is $-I_{mes}$, q is the electronic charge, k_B the Boltzmann constant, T the absolute temperature, n the ideality factor, and I_S the saturation current which can be expressed by the eq.:

$$I_S = AA^{**} T^2 \exp\left(\frac{-q\Phi_B}{k_B T}\right) \quad (5)$$

where A is the diode area, A^{**} the Richardson constant which is equal to $26.4 \text{ A}\cdot\text{cm}^{-2}\text{K}^{-2}$ for n-doped GaN [s18], and Φ_B the Schottky barrier height.

For each applied force, by fitting the linear region of the $\ln I$ - V curves, the ideality factor, n , and the Schottky barrier height, Φ_B , can be respectively calculated from slope and the y-intercept (corresponding directly to the logarithm of the saturation current).

The Cheung-Cheung theory [s19]:

Following this approach, which aims taking into account deviations from ideal behaviour, the I-V characteristics due to thermionic emission of the Schottky diode with the series resistance, R_s , can be expressed by Cheung functions given by eq. 6 and 7:

$$\frac{dV}{d\ln I} = n \frac{k_B T}{q} + IR_S \quad (6)$$

$$H(I) = n\Phi_B + IR_S \quad (7)$$

By fitting the curve $dV/d\ln I=f(I)$ to a straight line and by using eq. (6), n and R_s can be determined from the intercept and the slope of the line. Then by fitting the curve $H(I)=g(I)$ which gives a straight line, we can determine Φ_B and R_s from the slope and the y-axis intercept.

We note here that the calculations of the three diode characteristics have been performed for loading forces higher than the threshold ones, *i.e.* when the stable electric contact has been already formed.

[s17] D. K. Schroder, Semiconductor Material and Device Characterization. Wiley: New York, 2006.

[s18] P. Hacke, T. Detchprohm, K. Hiramatsu, N. Sawaki, Appl. Phys. Lett., 1993, 63, 2676.

[s19] S. K. Cheung, N. W. Cheung, Appl. Phys. Lett., 1986, 49, 85.